doi:10.3788/gzxb20154404.0423002

圆环杆与平板连杆的适合光路集成的二维正方晶格光子晶体

王晶晶,欧阳征标,文国华,黄浩,林密,王琼
(深圳大学 电子科学与技术学院 深圳市微纳光子信息技术重点实验室 太赫兹技术研究中心,广东 深圳 518060)

摘 要:提出了一种基于圆环杆与平板连杆的二维正方晶格光子晶体结构,讨论了绝对禁带的计算过程和各参数对绝对禁带宽度的影响.通过平面波展开法结合逐次逼近方法发现其最大绝对禁带相对值达到 19.026%,比采用圆柱杆和平板连杆结构的二维正方晶格光子晶体以及采用圆环杆但无连杆的二维正方晶格光子晶体的最大绝对禁带相对值分别提高 10.181%和 712.035 9%;圆环杆的外径、圆环的相对厚度以及连杆的宽度都存在一个最佳值,且连杆宽度对绝对禁带相对值的影响比较敏感.

关键词:光子晶体;光子禁带材料;集成光学材料
中图分类号:O436 **文献标识码**:A **文章编号**:1004-4213(2015)04-0423002-5

2D Square-lattice Photonic Crystal Based on Circular-ring Cylinders and Thin Cross Plates Suitable for Optical Integrated Circuits

WANG Jing-jing, OUYANG Zheng-biao, WEN Guo-hua, HUANG Hao, LIN Mi, WANG Qiong
(*THz Technical Research Center, Shenzhen Key Laboratory of Micro-nano Photonic Information Technology, College of Electronic Science and Technology, Shenzhen University, Shenzhen, Guangdong* 518060, *China*)

Abstract: A square-lattice photonic crystal structure was proposed based on circular-ring cylinders and thin cross plates. The calculation process and the influence of operating parameters on the absolute bandgaps were presented. It is demonstrated through plane wave expansion method combined with cut-and-try method that its maximum relative absolute photonic bandgap reaches 19.026%, which is 10.181% and 712.035 9% higher than that in a PhC made of solid cylinder and connecting veins and that in a PhC made of dielectric rings, respectively. And there exist optimum values for the outer radius of the circular-ring cylinders, the relative ring thickness, and the thickness of the cross plates. Furthermore, the influence of the thickness of the cross plates on the relative APBG is quite sensitive.

Key words: Photonic crystal; Photonic bandgap materials; Integrated optics materials
OCIS Codes: 230.5298; 050.5298; 160.5293; 130.3130

0 Introduction

Photonic Crystals (PhCs), as artificial electromagnetic and photonic materials with periodic refractive index distribution first predicted by Yablonovitch[1] and John[2], are promising candidates as platforms to build future microwave, infrared and photonic integrated devices with dimensions in the order of the operating wavelength[3], because PhCs have photonic bandgaps (PBGs) and thus the ability to control the motion of photons in these devices.

Foundation item: The National Natural Science Foundation of China (No. 61275043), the Shenzhen Science Bureau (No. CXB201105050064A)
First author: WANG Jing-jing (1989—), female, graduate student, M. S. degree, mainly focuses on large band gap of photonic crystal and components. Email: sanrojing@126.com
Supervisor (Contact author): OUYANG Zheng-biao (1963—), male, professor, Ph. D. degree, mainly focuses on photonic crystals and optoelectronic devices. Email: zbouyang@szu.edu.cn
Received: Oct. 10, 2014; **Accepted**: Dec. 11, 2014

A photonic bandgap is a property of PhCs, whereby light of certain frequencies is forbidden to propagate in the PhCs. For practical applications, three-dimensional photonic crystals exhibiting at least one Absolute PBG (APBG) at the telecommunication frequency band have been intensely looked for. However, three-dimensional photonic crystals are difficult to fabricate. Moreover, conventional integrated circuits are made using planar technology. Therefore two-dimensional (2D) photonic crystals combined with third-dimension confining measures are more useful in optical integrated circuits[4].

For applications, interest in seeking PhCs with large APBGs is ever lasting up to now because large APBGs can offer strong confinement of waves, low transmission loss, wide operating bandwidth, good tolerance for the technological error and flexibility of designing photonic devices[5-9]. Among the PhCs in various kinds of lattices, PhCs in square lattice are more easily and economically fabricated[10]. Moreover, PhCs in square lattice can simplify the optical circuits and increase the scale of integration in many cases. Therefore, seeking square-lattice PhCs with large APBGs is important and interesting. In this paper, we present a square-lattice PhC, in which the unit cell is made of a hollow cylinder and four vertically arranged connecting plates. We find that such a square-lattice PhC based on silicon material has a relative maximum APBG of 19.026%, which is wider than that in other square PhCs reported. The so called relative APBG is defined as the APBG divided by the central frequency of the PBG.

1 Description of the proposed PhC and method for seeking the largest PBG

Fig. 1 shows the overview and the structure of the 2D square-lattice PhC proposed. From Fig. 1 we can see that, in the unit cell there is a hollow cylinder and four connecting plates arranged uniformly around the cylinder in 90°. The hollow cylinder and the connecting plates have high dielectric constant and the background material has a low dielectric constant. As an example in this paper, the high and low dielectric constant material are chosen as silicon (dielectric constant of 3.4) and air (dielectric constant of 1), respectively. One can imagine that the hollow cylinders in the whole PhC are connected together by the plates in three-dimensional view——this is why we call the plates as connecting plates.

According to the unit cell and the type of the lattice, we can calculate the APBG. As shown in Fig. 1 (b), there are three parameters we need to scan: D, R and r, which are the width of the plates, the outer radius, and the inner radius, respectively. For convenience, we scan T, defined as $T=(R-r)/R$, instead of r. Note that the length of the connecting plates is equal to $(0.5a_c-R)$, where a_c is the lattice constant.

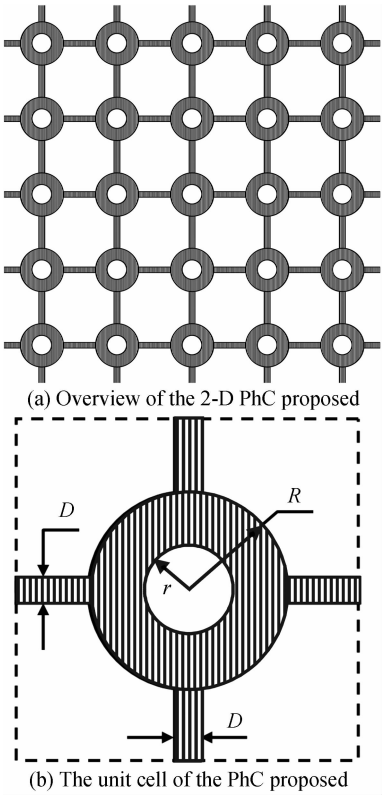

Fig. 1 The 2D square-lattice PhC proposed where the filled and unfilled area are silicon and air, respectively

We used plane-wave expansion method to calculate the band structure and the relative APBG through commercial software Rsoft BandSolve module. We adopted the cut-and-try method for further scanning to get the largest relative APBG in the PhC. The cut-and-try process is shown in Fig. 2. For simplicity, we use (a,b,c) to replace (D,R,T) in the following. For the first step, we scan (a,b,c) in their allowable range of value. Then we can find out that there is a first-step widest relative APBG r_{g1}. The corresponding parameters are (a_0,b_0,c_0). After that, we go to the second step. We first keep $(a,b)=(a_0,b_0)$ and scan parameter c, obtaining c_1 corresponding to a new widest relative APBG. Then we keep $(a,c)=(a_0,c_1)$ and scan b, obtaining b_1 corresponding to a further new widest relative APBG. Then we keep $(b,c)=(b_1,c_1)$ and scan a, obtaining a_1 corresponding to the second-step widest relative APBG r_{g2}. Following the second step, we go to check the inequality $2|r_{g2}-r_{g1}|/|r_{g2}+r_{g1}|<1\%$. If this inequality is not satisfied, we set the value of r_{g1} to be r_{g2} just now obtained and we go to do the second-step scanning (indicated by light-green-filled dashed rectangular region in Fig. 2) again and get a new r_{g2} and check the inequality again. If the inequality is satisfied,

we end the cut-and-try process. Therefore we can obtain the Maximum Relative APBG (MRA).

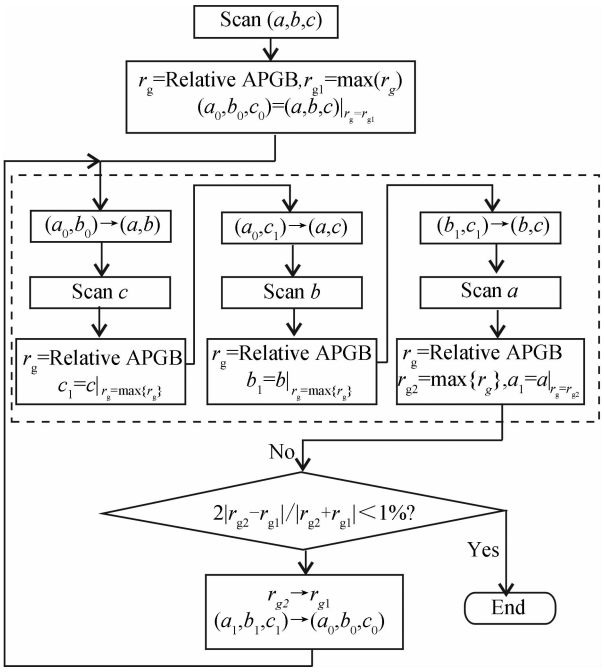

Fig. 2 Flowchart of seeking the widest absolute relative APBG

2 Results and discussions

2.1 Results of simulations

2.1.1 *The maximum relative absolute APBG*

For the structure proposed, there are three operating parameters (D, R, T) that influence the band structure and PBG. We first need to determine the scanning range of these parameters. Without loss of generality, we suppose the lattice constant $a_c=1$ μm in the following when not specified. Then we have $R\leqslant 0.5$ μm. By experience, the PBG would be quite small if $R<0.1$ μm. So, the maximum scanning range for R can be chosen as 0.1 μm～0.5 μm. On the other hand, we note that the connecting plates are used mainly to modify the TM band structure to obtain large APBG. So, to have small influence on the TE PBG, the width of the connecting plates D can only take small values. Thus we take the scanning range for D as 0.01 μm～0.1 μm. Finally, noting that hollow cylinder can be a very thin ring ($T\approx 0$) or a very thick ring ($T\approx 1$), we choose the scanning range of T as 0.01～0.99.

With the chosen range of the three operating parameters, we can obtain the MRA to be 19.026% using the cut-and-try method described in Sec. 1. The corresponding optimum operating parameters are as follows: $D/a_c=0.049$, $R/a_c=0.296$, and $T=0.838$. The corresponding gap map is shown in Fig. 3 where the regions filled with vertical lines, horizontal lines, and black color indicate the TE, TM and absolute PGB, respectively.

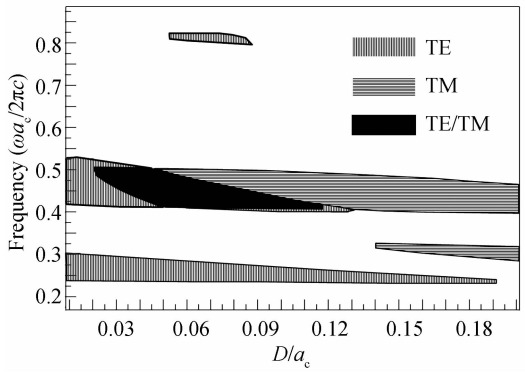

Fig. 3 The optimum TE/TM PBG

We note that the MRA obtained for the proposed PhC is 118.9% times of that in the square PhC reported in Ref. [5], where the MRA is 16%. The reason behind the promotion of the relative APBG is as follows. Larger radius of the cylinders is favorable for wider TM PBG. However, larger radius leads to large filling factor for solid cylinders, and filling factor greater than a certain value would lead to a decrease of the TE PBG. However, for hollow cylinders, the filling factor can be controlled by the empty region in the hollow cylinder, so that a higher value of the relative APBG can be obtained in our proposed PhC. It is noted that the filling factor F can be expressed as

$$F=a_c^{-2}\left[4D\left(\frac{a_c}{2}-R\right)+\pi(R^2-r^2)\right]= a_c^{-2}\left[4D\left(\frac{a_c}{2}-R\right)+\pi(2-T)TR^2\right] \quad (1)$$

for $D\ll R$ in the structure shown in Fig. 1.

For more details about the optimum operating state, the corresponding band structure and appearance of the unit cell is plotted in Fig. 4. From Fig. 4 we can see that the APBG is from 0.412 67 to 0.499 43 of normalized frequency $f=\omega a_c/2\pi c=a_c/\lambda$, where ω is the angular frequency and c is the speed of light in free space. The normalized center frequency is 0.456 05. If we take the lattice constant as 0.294 226 μm, we can get the center λ to be 1.55 μm which is the optical communication wavelength.

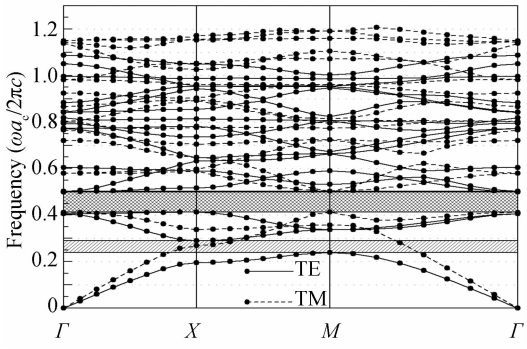

Fig. 4 Photonic band structure for TE (solid lines) and TM (dashed lines)

2.1.2 *Influence of operating parameters on the maximum relative APBG*

Now we move to study the influence of the three operating parameters on the relative APBG.

The influence of T on the relative APBG is showed in Fig. 5. When R and D are fixed, larger T corresponds to smaller r, i. e., the filling factor increases with T. From Fig. 5, we can see that the relative APBG increases with T for T varies from 0.277 27 to 0.838 and there is an optimum T (=0.838) at which there is an MRA (=19.026%) for $D/a_c=0.049$ and $R/a_c=0.296$.

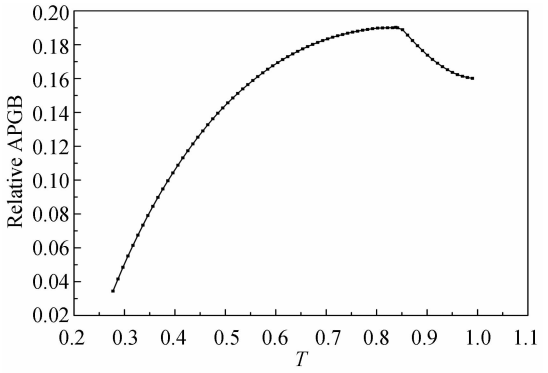

Fig. 5 Influence of T on the relative APBG for $D=0.049$ μm and $R=0.296$ μm

The influence of the outer radius R of the hollow cylinder on the relative APBG is shown in Fig. 6. From Fig. 6 we can see that there exists an optimum R that corresponds to an MRA. This can also be understood by noting that R relates directly to the filling factor, of which a certain value leads to the MRA.

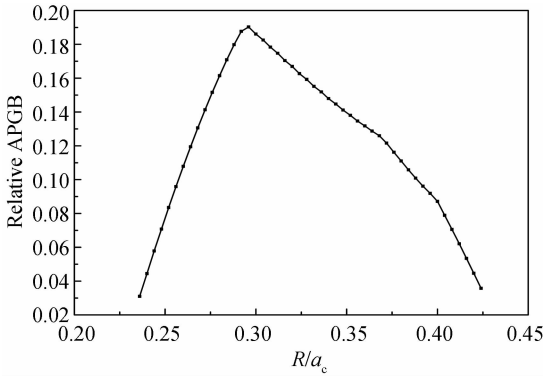

Fig. 6 Relative APBG versus the outer radius R of the hollow cylinder for $D/a_c=0.049$ and $T=0.838$

The influence of the thickness D of the connecting plates on the relative APBG is shown in Fig. 7. From Fig. 7 we see that there exists also an optimum value of D/a_c (=0.049) that corresponds to an MRA of 19.026%. Furthermore, we can see that the range of D for obtaining the APBG is very narrow. We may understand this by noting: 1) If the connecting plates are too thin, the structure is equivalent to PhCs made of hollow cylinders which have just a small relative APBG; 2) The filling factor increases rapidly with the increase of D as there are four plates in each unit cell in the PhC, so that the APBG will be very sensitive to D.

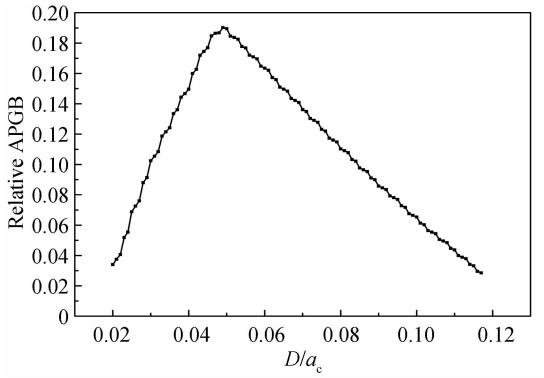

Fig. 7 Relative APBG versus the thickness D of the connecting plates for $T=0.838$ and $R/a_c=0.296$

Comparing Figs. 5～7, we can see that the relative APBG in Fig. 5 is less sensitive to T. This is understandable because T influences the filling factor through $(2-T)T$ as can be seen from Eq. (1), while D and R influence the filling factor through $4D$ and (πR^2-4DR), respectively.

2.2 Comparison with other structures

For comparison, we used the cut-and-try method introduced in Section 1 to calculate the MRA of two related PhCs: a) a PhC made of solid cylinders and cross veins[5]; b) a PhC made of circular rings or hollow cylinders[11]. The results are shown in Table 1. For convenience of comparison, Table 1 also shows the RMRA, which is defined as the ratio of the MRA in our structure indicated in Fig. 1 to that in other structures in literatures.

Table 1 Comparison of MRAs in a few related 2D PhCs

Structure	MRA	RMRA
Structure in Fig. 1	19.026%	100%
Structure in Ref. [5]	17.268%	110.181%
Structure in Ref. [11]	2.343%	812.036%

From Table 1, we can see that our structure's MRA is 10.181% and 712.036% higher than that in Refs. [5] and [11], respectively. It is noted that the reported MRA for the PhC proposed in Ref. [5] was 16%, less than the value 17.249% obtained using the cut-and-try method introduced in Section 1 in this paper for the same operating parameters as that in Ref. [5]. This shows that the cut-and-try method introduced in this paper is a powerful method.

The physical mechanism is: The introduction of both connecting plates and holes in the cylinders increases the effective refractive index for TM waves while imposes small influence on the effective refractive index for TE waves, so that the relative APBG in our PhC is the largest because the PhCs presented in Refs.

[5] and [11] only benefit from one of the two factors——the PhC in Ref. [5] has no hole in the cylinders, while the PhC in Ref. [11] has no connecting plates.

Finally, we point out that specific measures of technological aspects have to be taken because the diameter of the hole in the hollow cylinders is relatively small. For fabrication, we can consider the following methods: 1) laser-beam, ion-beam or electron-beam drilling; 2) melting-of-template method——using a material with a melting point lower than that of the hollow cylinder dielectric material to create first an inverse-structure template of the PhC, then filling the desired high refractive index medium (such as silicon) into the template, and finally removing the template material through melting at a proper high temperature; 3) dissolving-of-template method: first using a material soluble in water (oil, acid, or alkali) to produce an inverse-structure template of the PhC, then filling the desired high refractive index medium (such as silicon) into the template, and finally removing the template material by water (oil, acid, or alkali); 4) combustion-of-template method: first using a material with a burning point below that of the hollow cylinder dielectric material to create an inverse-structure template of the PhC, then filling the desired high refractive index medium (such as silicon) into the template, and finally removing the template by combustion of the template material. We can choose the proper fabrication method according to the dielectric material of photonic crystal and the operating at different wavelengths.

3 Conclusions

We have proposed a 2D square-lattice PhC with its unit cell made of hollow cylinders and connecting plates. It is demonstrated by PWE method and the powerful cut-and-try method to have a very large relative APBG of 19.026%, which is 10.181% and 712.035 9% higher than that in a PhC made of solid cylinder and connecting veins and that in a PhC made of dielectric rings, respectively. It is further found that there exist optimum values for the outer radius of the circular-ring cylinders, the relative ring thickness, and the thickness of the cross plates. Moreover, the influence of the thickness of the cross plates on the relative APBG is quite sensitive. The mechanism behind the promotion of the relative APBG is discussed also. The proposed PhC can find wide applications in optical integrated circuits.

Reference

[1] YABLONOVITH E. Inhibited spontaneous emission in solid-state physics and electronics [J]. *Physical Review Letters*, 1987, **58**(20): 2059-2062.

[2] JOHN S. Strong localization of photons in certain disordered dielectric superlattices [J]. *Physical Review Letters*, 1987, **58**(23): 2846-2489.

[3] JOANNOPOULOS J D, VILLENEUVE P R, FAN S. Photonics crystals: putting a new twist on light [J]. *Nature*, 1997, **386**: 143-149.

[4] VILLENEUVE P, PICHE M. Photonic band gaps in two-dimensional square lattices: Square and circular rods [J]. *Physical Review B*, 1992, **46**(8): 4973-4975.

[5] MA Tian-xue, WANG Yue-sheng, ZHANG Chuan-zeng. Investigation of dual photonic and phononic bandgaps in two-dimensional phoxonic crystals with veins [J]. *Optics Communications*, 2014, **312**: 68-72.

[6] FARAON A, FUSHMAN I, ENGLUND D, *et al*. Dipole induced transparency in waveguide coupled photonic crystal cavities [J]. *Optics Express*, 2008, **16**(16): 12154.

[7] KONG F, SAITOH K, MCCLANE D, *et al*. Mode area scaling with all-solid photonic bandgap fibers [J]. *Optics Express*, 2012, **20**(24): 26363.

[8] ERDIVEN U, KARADAG F, KARAASLAN M, *et al*. Photonic band gap engineering in two-dimensional photonic crystals and iso-frequency contours [J]. *Journal of Electromagnetic Waves and Applications*, 2014, **28**(2): 253-263.

[9] FENG Zhi-fang, ZHANG Dan-dan, ZHAN Ke-tao, *et al*. The influence of structural/shape anisotropy in 2-D photonic crystals [J]. *Physica B: Condensed Matter*, 2013, **422**: 6-11.

[10] HO Hong-fa, CHAU Yuan-fong, YEH Hsiao-yu, *et al*. Absolute bandgap arising from the effects of hollow, veins, and intersecting veins in a square lattice of square dielectric rods photonic crystal [J]. *Applied Physics Letters*, 2011, **98**(26): 263115.

[11] LIU Dan, LIU Hui, GAO Yi-hua. Photonic band gaps in square photonic crystal slabs of core - shell-type dielectric nanorod heterostructures [J]. *Solid State Communications*, 2013, **172**: 10-14.